Analysis of Pressure Balanced MEMS Valves

Fuqian Yang and Imin Kao
Systems Engineering and Integration Laboratory
Department of Mechanical Engineering
SUNY at Stony Brook, Stony Brook, NY 11794-2300
Email: yang@mal.eng.sunysb.edu

Abstract

Based on simple plate theory and the Bernoulli equation, the effect of fluid flow on the deformation of fluid driven MEMS diaphragm microvalve is investigated analytically and numerically. The static instability of such a microsystem is demonstrated with both analytical and numerical solutions. Theoretical formula is presented for prediction of the limit flow velocity at which the pressure difference across the diaphragm is positive over the whole MEMS diaphragm. In addition, static stiction phenomena is analyzed and a closed form solution of the relation between the contact zone and the external pressure is obtained. The results provide important information of parameters in the design of MEMS diaphragm valve and can be used as a basis in the mechanical design of such valves.

Keywords: fluid-structure interaction, plate theory, Bernoulli equation, MEMS valve

INTRODUCTION

Miniaturization of mechanical systems promises unique opportunities for progress of engineering and technology in new directions. Based on the microelectronic fabrication technology, extensive microelectromechanical systems and devices, such as microvalves, microchannels, microdiffusers, microgenerators, and micromotors etc. [1], have been built. Such devices are inherently smaller, lighter, faster, and usually more precise than their macroscopic counterparts. Some of these components have been successfully combined to realize micromechanical systems. A microsystem is a complex miniaturized array of materials such as silicon, metals and plastic. It is obvious that successful microfabrication technology requires a detailed knowledge of packaging, materials, device behavior, reliability, and an understanding of current fabrication technology. Therefore, an effort on modeling MEMS micromechanical behavior under different working environments, which will provide a sound basis for the application of MEMS, is needed.

The desired general features for a MEMS valve include:

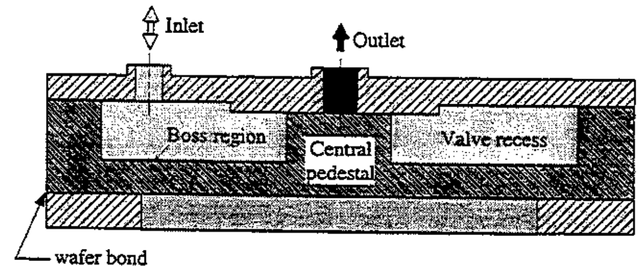

Figure 1: A schematic diagram of MEMS pressure-balanced diaphragm valves

1) quick response,
2) low driving energy,
3) low energy consumption,
4) stable temperature characteristics,
5) small size and weight,
6) no degradation and aging in use,
7) no negative environmental effects.

Several kind of MEMS microvalves driven by different mechanism have been reported in the literature. Most of them consists of a diaphragm made from either nickel [2] or silicon [3]. The mechanism includes, electromagnetic [2], [3], electric [4], thermal [5], and pneumatic [6]. Among these mechanisms, the pressure balanced MEMS microvalves are attractive because of the low energy consumption in the operation. Here we briefly describe the basic working mechanism of the pressure balanced MEMS microvalve (for detail see Huff and Schmidt [6]). Figure 1 shows a schematic diagram of microvalve. Fluid such as air, water, etc., flows into the microchamber between the valve and a substrate,which generates a pressure difference across the valve and provides a driving force to control the motion of the valve. Consequently, the total force necessary to actuate the valve can be designed to be only a small fraction of the total pressure of the fluid by properly sizing the top and bottom surfaces of the microstructure [6]. Without considering the effect of fluid flow on the pressure distribution across the valve, Huff et al. [7] have analyzed the mechanical behavior of the microvalve on the basis of laminar flow

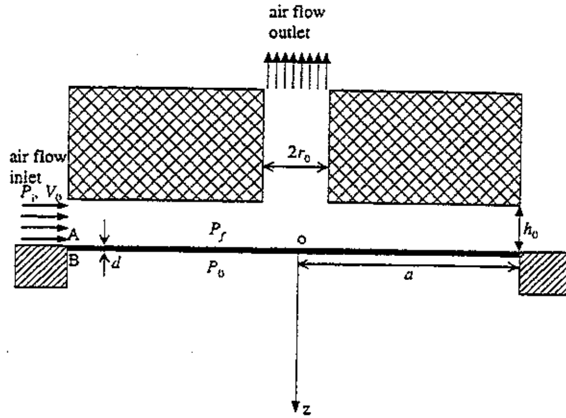

Figure 2: A model of pressure-balanced microvalves

and simple plate theory. However, when fluid flow occurs, the microvalve surface is subjected to non-uniform pressure, which is a function of fluid velocity.

The motivation of this work is to develop a quasistatic model for the pressure-balanced type of MEMS microvalves by accounting for the fluid-structure interaction. This model provides us a method to design and investigate the effect of fluid flow on the reliability of these devices.

STATIC MODELING OF MEMS MICROVALVE

Figure 2 shows the model of a pressure-balanced MEMS microvalves. Fluid flows into the microchannel from inlet A and exits at outlet B. The fluid is assumed to be incompressible and inviscid and the microvalve elastic. For simplicity, the wall is treated as a rigid body. Under small deformation, simple plate theory is used. The governing equation of the microvalve deflection is

$$\nabla^4 w = \frac{\Delta P}{D} \tag{1}$$

where w is the valve transverse deflection, ΔP $(= P_f - P_0)$ is the pressure difference across the microvalve, P_f is the hydrostatic pressure in the fluid, P_0 is the constant pressure applied onto the valve on the side of B, and D=$Ed^3/12(1-\nu^2)$ the bending stiffness, E is Young's modulus, d is the thickness of the microvalve, and ν is the Poisson ratio. For the MEMS microvalve shown in Figure 2, the boundary conditions are

$$w = \frac{dw}{dr} = 0 \qquad \text{at } r = a \tag{2}$$

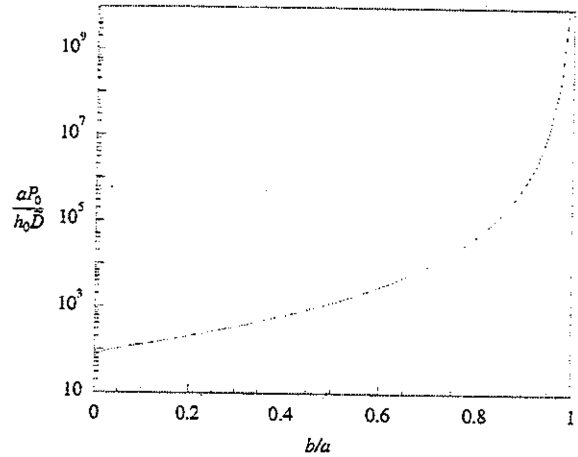

Figure 3: The relation between the contact radius and the applied pressure

The fluid flow satisfies the Bernoulli equation

$$\frac{P_f}{\rho} + \frac{V^2}{2} = constant \tag{3}$$

where ρ is the fluid density, and V is the flow velocity. Before solving the above equations, we introduce the following dimensionless variables

$$\tilde{r} = r/a,\ \tilde{w} = w/a,\ and\ \tilde{D} = \frac{E}{12(1-\nu^2)}\left(\frac{d}{a}\right)^3 \tag{4}$$

CONTACT PROBLEM IN MEMS MICROVALVE

Before solving the above equations relating the deflection of microvalve, we first consider the contact problem occurring in MEMS microvalve systems. To close the valve, a pre-applied pressure (P_0) shown in Figure 2 is applied to the valve on the side of B, while the pressure and fluid velocity on the side A is set to zero. This forces the valve to contact the substrate and block the fluid flow. Under this condition, the contact radius (b) between the valve and the substrate is a function of the distance h_0 and the pressure P_0. At the edge of the contact zone, the boundary conditions are

$$w = -h_0 \text{ and } \frac{dw}{dr} = \frac{d^2w}{dr^2} = 0 \qquad \text{at } r = b \tag{5}$$

with b to be determined. The first condition indicates the constraint on the deflection of the valve, the second means that the slope of the valve at the edge of the contact zone is zero, and the third implies the moment (M_r) is zero. For the constant pressure difference

($\Delta P = -P_0$), the solution of equation (1) is

$$\bar{w} = c_1 + c_2 \ln \bar{r} + c_3 \bar{r}^2 + c_4 \bar{r}^2 \ln \bar{r} - \frac{P_0 \bar{r}^4}{64 \bar{D}} \tag{6}$$

where c_i (I=1, ..., 4) are determined by the boundary conditions, which will not be given here because we are only interested in the size of the contact zone. Using the boundary conditions (2) and (5), the dependence of the contact radius on the valve stiffness, the gap between the valve and the substrate, and the external pressure is

$$\frac{aP_0}{h_0 \bar{D}} = \frac{-64 + 64\lambda^2 - 128 \ln \lambda}{f(\lambda)} \tag{7}$$

and

$$f(\lambda) = -3 + 7\lambda^2 - 5\lambda^4 + \lambda^6 - 2 \ln \lambda \\ -4\lambda^2 \ln \lambda + 6\lambda^4 \ln \lambda - 8\lambda^4 \ln^2 \lambda \tag{8}$$

where $\lambda = b/a$. Figure 3 shows the effect of the pressure on the contact zone under different gap. The contact zone increases with the pressure, as expected; while it decreases with increasing the microvalve stiffness. This suggests that the stiction problem occurred in microsystems may be reduced by increasing the valve stiffness.

DEFLECTION OF MEMS MICROVALVE

When pressure higher than the pressure (P_0) is applied onto the microvalve on the side A, the microvalve is opened. Fluid flows from the inlet to outlet and a pressure field is generated on the side A of the valve. The deflection of the MEMS microvalve is described by equations (1-3). For inlet pressure of P_i and fluid flow velocity of V_0, equation (3) gives

$$\frac{P_f}{\rho} + \frac{V^2}{2} = \frac{P_i}{\rho} + \frac{V_0^2}{2} \tag{9}$$

For incompressible fluid, the volume conservation gives

$$V = \frac{a h_0 V_0}{r h} \qquad \text{for } r_0 \le r \le a \tag{10}$$

the fluid velocity between the valve and the substrate, where h is the distance between the valve and the substrate at the radius r. Substituting equation (10) into equation (9), the pressure due to the fluid flow is

$$P_f = P_i + \frac{\rho V_0^2}{2} \left[1 - \left(\frac{a h_0}{r h} \right)^2 \right] \qquad \text{for } r_0 \le r \le a \tag{11}$$

For simplicity, the pressure applied onto the valve at the outlet is assumed to be a constant

$$P_f = P_f|_{r=r_0} \qquad \text{for } r < r_0 \tag{12}$$

Equations (11) and (12) indicate that, to generate positive pressure difference for fluid to flow, it requires

$$P_i + \frac{\rho V_0^2}{2} \left[1 - \left(\frac{a h_0}{r_0 h} \right)^2 \right] > 0 \tag{13}$$

This imposes a limitation on the highest fluid velocity to maintain positive pressure difference over the diaphragm surface for a given geometrical configuration of the MEMS microvalve or the geometrical constraint on the valve for given pressure and fluid velocity. Substituting equations (11) and (12) into equation (1), we have

$$\nabla^4 w = \frac{1}{D} \left\{ P + \frac{\rho V_0^2}{2} \left[1 - \left(\frac{a h_0}{r h} \right)^2 \right] \right\} \text{for } r_0 \le r \le a \tag{14}$$

$$\nabla^4 w = \frac{1}{D} \left\{ P + \frac{\rho V_0^2}{2} \left[1 - \left(\frac{a h_0}{r_0 h} \right)^2 \right] \right\} \quad \text{for } r < r_0 \tag{15}$$

where $P = P_i - P_0$ and $h = h_0 + w$. Equations (14) and (15) are nonlinear differential equation, which can not solved analytically. A numerical method will be used to analyze the relation among the microvalve deflection, the pressure P, and the fluid velocity.

There are different numerical methods, such as shooting method, spectral method, finite difference method, variational method, and finite element method, that can be used to solve the above equations. Here, we use the superposition method. Using the result for a ring load applied symmetrically onto the valve surface [8], the deflection of the microvalve due to the pressure given by equations (11) and (12) is, for $0 \le r \le r_0$

$$\begin{aligned} w \;=\; & (P + \frac{\rho V_0^2}{2}) \frac{(a^2 - r^2)^2}{64 D} - \frac{\rho V_0^2}{8D} \left(\frac{a}{r_0} \right)^2 \\ & \left[\int_0^r [(a^2 - r^2) \frac{a^2 + \breve{r}^2}{2a^2} + (\breve{r}^2 + r^2) \ln \frac{r}{a}] \right. \\ & \left(\frac{h_0}{h_0 + w(\breve{r}_0)} \right)^2 \breve{r} d\breve{r} + \int_r^{r_0} [(a^2 + r^2) \frac{a^2 - \breve{r}^2}{2a^2} \\ & \left. + (\breve{r}^2 + r^2) \ln \frac{\breve{r}}{a}] \left(\frac{h_0}{h_0 + w(\breve{r}_0)} \right)^2 \breve{r} d\breve{r} \right] \\ & - \frac{\rho a^2 V_0^2}{8D} \int_{r_0}^a [(a^2 + r^2) \frac{a^2 - \breve{r}^2}{2a^2} + (\breve{r}^2 + r^2) \ln \frac{\breve{r}}{a}] \\ & \left(\frac{h_0}{h_0 + w(\breve{r})} \right)^2 \frac{d\breve{r}}{\breve{r}} \end{aligned} \tag{16}$$

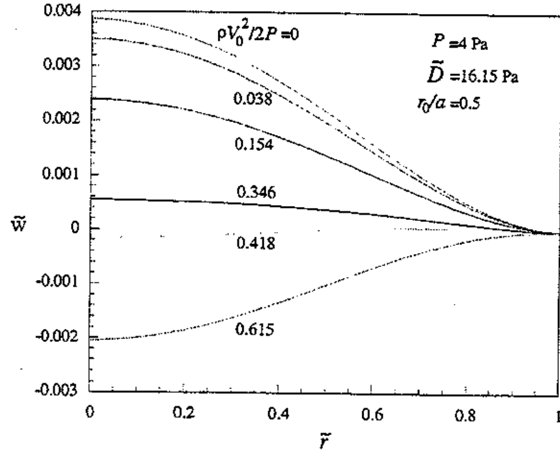

Figure 4: Effect of the air speed on the deflection of the valve for the limiting condition

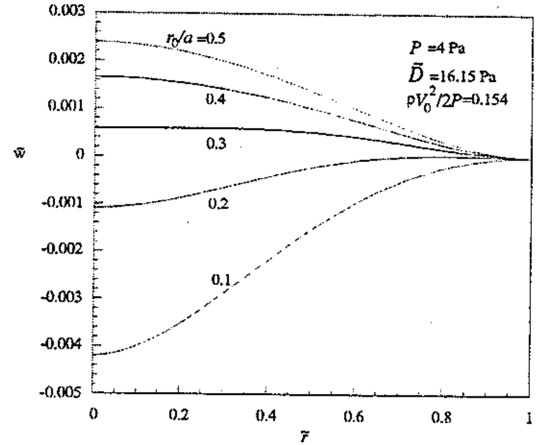

Figure 5: Effect of the outlet radius on the deflection of the valve for the limiting condition

and for $r_0 \leq r \leq a$

$$\begin{aligned} w &= (P+\frac{\rho V_0^2}{2})\frac{(a^2-r^2)^2}{64D} - \frac{\rho V_0^2}{8D}\left(\frac{a}{r_0}\right)^2 \\ & \int_0^{r_0}[(a^2-r^2)\frac{a^2+\tilde{r}^2}{2a^2}+(\tilde{r}^2+r^2)\ln\frac{r}{a}] \\ & \left(\frac{h_0}{h_0+w(\tilde{r}_0)}\right)^2\tilde{r}d\tilde{r} - \frac{\rho a^2 V_0^2}{8D}\left[\int_{r_0}^{r}[(a^2-r^2)\right. \\ & \frac{a^2+\tilde{r}^2}{2a^2}+(\tilde{r}^2+r^2)\ln\frac{r}{a}] \\ & \left(\frac{h_0}{h_0+w(\tilde{r})}\right)^2\frac{d\tilde{r}}{\tilde{r}}+\int_r^a[(a^2+r^2)\frac{a^2-\tilde{r}^2}{2a^2} \\ & \left.+(\tilde{r}^2+r^2)\ln\frac{\tilde{r}}{a}]\left(\frac{h_0}{h_0+w(\tilde{r})}\right)^2\frac{d\tilde{r}}{\tilde{r}}\right] \end{aligned} \tag{17}$$

which is an integral equation to be solved numerically.

Limiting Case

Considering the limiting situation, $w << h_0$, the pressure distribution can be approximated as the following

$$P_f = P_i + \frac{\rho V_0^2}{2}\left[1-\left(\frac{a}{r}\right)^2\right] \qquad \text{for } r_0 \leq r \leq a \tag{18}$$

$$P_f = P_i + \frac{\rho V_0^2}{2}\left[1-\left(\frac{a}{r_0}\right)^2\right] \qquad \text{for } r < r_0 \tag{19}$$

The deflection of the microvalve is, for $0 \leq r \leq r_0$

$$\begin{aligned} w &= (P+\frac{\rho V_0^2}{2})\frac{(a^2-r^2)^2}{64D} - \frac{\rho V_0^2}{8D}\left(\frac{a}{r_0}\right)^2 \\ & \left[\frac{r^4}{16}+\frac{a^2r_0^2}{4}-\frac{3r_0^4}{16}-\frac{r^2r_0^4}{8a^2}+\frac{(r_0^2+2r^2)r_0^2}{4}\ln\frac{r_0}{a}\right] \\ & -\frac{\rho a^2 V_0^2}{8D}\left[-\frac{2a^2+r^2}{4}-\frac{(a^2+r^2)}{2}\ln\frac{r_0}{a}\right. \\ & \left.+\frac{r_0^2(2a^2+r^2)}{4a^2}-\frac{r_0^2}{2}\ln\frac{r_0}{a}-\frac{r^2}{2}\left(\ln\frac{r_0}{a}\right)^2\right] \end{aligned} \tag{20}$$

and for $r_0 \leq r \leq a$

$$\begin{aligned} w &= (P+\frac{\rho V_0^2}{2})\frac{(a^2-r^2)^2}{64D} - \frac{\rho V_0^2}{8D}\left(\frac{a}{r_0}\right)^2 \\ & \left[\frac{r_0^4(a^2-r^2+2a^2\ln(r/a))}{8a^2}\right. \\ & \left.+\frac{r_0^2(a^2-r^2+2r^2\ln(r/a))}{4}\right] \\ & -\frac{\rho a^2 V_0^2}{8D}\left[-\frac{a^2-r^2}{2}+\frac{a^2+r^2}{2}\ln\frac{a}{r}\right. \\ & -\frac{r^2}{2}\left(\ln\frac{r}{a}\right)^2-\frac{r_0^2(a^2-r^2+2a^2\ln(r/a))}{4a^2} \\ & \left.+\frac{a^2-r^2+2r^2\ln(r/a)}{2}\ln\frac{r}{r_0}\right] \end{aligned} \tag{21}$$

Assume that the microvalve is made of silicon and the fluid is air and use the parameters, E=169 GPa and ν=0.358 along the (111) direction of single crystalline silicon [9], ρ = 1.23 kg/mm^3 of air at 15 ^oC [10], and d/a=0.01. The deflection of the microvalve under different conditions is plotted in Figures 4 and 5. For the same geometrical configuration, Figure 4 shows that the deflection of MEMS valve first decreases with increasing the fluid velocity then the deflection direction reverses. The distance between the valve and the substrate decreases with increasing speed and may cause the block of the air flow and instability of the microvalve system. Similar to the increase of the air speed, the decrease

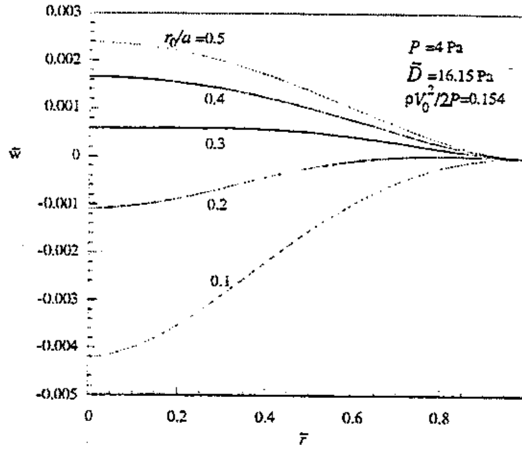

Figure 6: Effect of the air speed on the deflection of the valve

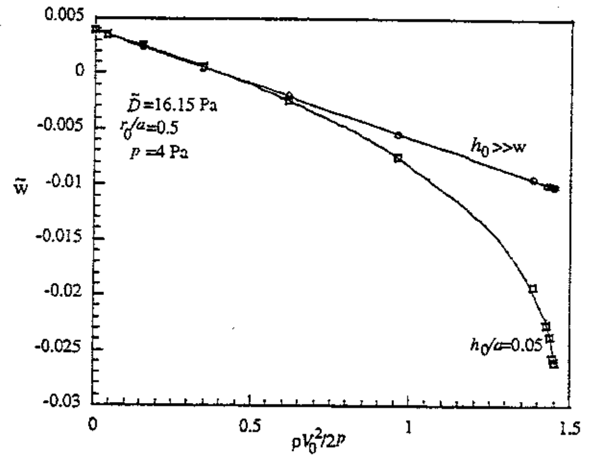

Figure 7: Dependence of the valve center deflection on the air speed

of the outlet radius also causes the reverse deflection of the microvalve and increases the possibility of the in-use stiction as shown in Figure 5.

Numerical Calculation

Equations (16) and (17) constitute a set of nonlinear integral equations. Before solving them, the equation is simplified as below, for $0 \le r \le r_0$

$$\begin{aligned} w \;=\; & (P+\frac{\rho V_0^2}{2})\frac{(a^2-r^2)^2}{64D} - \frac{\rho V_0^2}{8D}\left(\frac{a}{r_0}\right)^2 \\ & \left(\frac{h_0}{h_0+w(r_0)}\right)^2 \left[\frac{r^4}{16}+\frac{a^2 r_0^2}{4}-\frac{3r_0^4}{16}-\frac{r^2 r_0^4}{8a^2} \right. \\ & \left. +\frac{(r_0^2+2r^2)r_0^2}{4}\ln\frac{r_0}{a}\right] \\ & -\frac{\rho a^2 V_0^2}{8D}\int_{r_0}^{a} [(a^2+r^2)\frac{a^2-\bar{r}^2}{2a^2} \\ & +(\bar{r}^2+r^2)\ln\frac{\bar{r}}{a}]\left(\frac{h_0}{h_0+w(\bar{r})}\right)^2\frac{d\bar{r}}{\bar{r}} \end{aligned} \tag{22}$$

and for $r_0 \le r \le a$

$$\begin{aligned} w \;=\; & (P+\frac{\rho V_0^2}{2})\frac{(a^2-r^2)^2}{64D} - \frac{\rho V_0^2}{8D}\left(\frac{a}{r_0}\right)^2 \\ & \left(\frac{h_0}{h_0+w(r_0)}\right)^2 \left[\frac{r_0^4(a^2-r^2+2a^2\ln(r/a))}{8a^2} \right. \\ & \left. +\frac{r_0^2(a^2-r^2+2r^2\ln(r/a))}{4}\right] - \frac{\rho a^2 V_0^2}{8D} \\ & \left[\int_{r_0}^{r} [(a^2-r^2)\frac{a^2+\bar{r}^2}{2a^2}+(\bar{r}^2+r^2)\ln\frac{r}{a}]\right. \\ & \left(\frac{h_0}{h_0+w(\bar{r})}\right)^2\frac{d\bar{r}}{\bar{r}}+\int_{r}^{a} [(a^2+r^2)\frac{a^2-\bar{r}^2}{2a^2} \\ & \left. +(\bar{r}^2+r^2)\ln\frac{\bar{r}}{a}]\left(\frac{h_0}{h_0+w(\bar{r})}\right)^2\frac{d\bar{r}}{\bar{r}}\right] \end{aligned} \tag{23}$$

The iterative method is used here to obtain the numerical solution. To implement this method, an initial deflection based on equations (22) and (23) is employed to calculate the possible valve deformation as follows

$$w_n = f(w_{n-1}) \qquad \text{for } (n=1,2,3,...) \tag{24}$$

where the function is given in equations (16) and (17). The calculation will continue until $|w_n - w_{n-1}|$ $(0 \le r \le a)$ reaches the allowable value. The parameters used here are the same as those in the above section but we also consider the dependence of the valve deflection on the distance between the valve and the substrate.

To analyze the effect of the flow speed on the valve deflection, several different speeds are used. Figure 6 shows the valve deflection for h_0/a=0.05, $d/a = 0.001$, and $r_0/a = 0.5$. The microvalve deformation has the same trend as that in the limiting case. A reverse deflection of the valve is found, which might cause the unstable operation of the microsystem at high fluid speed. Together with the data from the limiting case in Figure 7, the effect of air flow velocity on the center deflection of the valve is shown. A linear relationship between the deflection and the kinetic energy of the air is observed for the limiting case, which is expected from the linear plate theory. The deflection for the limiting case is always smaller without considering the effect of distance between the valve and the substrate. When the reverse deflection of the diaphragm valve reaches about 10% of the distance, the deflection of the diaphragm is a nonlinear function of the air kinetic energy. Further

increase in the gas kinetic energy (air speed) beyond certain value will increase the reverse deflection of the valve and lead to the collapse of the microvalve at a critical air speed. For example, this occurs at $\rho V_0^2/2p > 1.4$ for the above configuration. This may cause the system to fail. If we continue to increase the gas kinetic energy, nonlinear large deformation plate theory should be used. However, the large deformation will lead to the fracture of the microvalve due to the brittle properties of the valve materials. Therefore, the operation range of the air speed is approximately limited by equation (13).

CONCLUSION

Based on simple plate theory and the Bernoulli equation, the effect of inviscid fluid flow on the deformation of the microvalve is analyzed. It turns out that, if the pressure difference applied onto the MEMS microvalve surface is positive in the direction of opening the valve, the microsystem can work properly. Otherwise, a collapse phenomenon will occur and may cause the failure of the system under certain working conditions, such as high fluid speed, small outlet radius, and the small gap between the valve and the substrate. For a given geometrical configuration, the constraint on the fluid pressure and its speed is given in equation (13), at which the pressure difference across the MEMS diaphragm is positive. The analysis provides us with a sound mechanical basis for designing and fabricating MEMS microvalves.

REFERENCES

[1] L. O'Connor. Mems: Microelectromechanical systems. *Mechanical Engineering*, pages 40–47, February 1992.

[2] S. C. Terry, J. H. Jerman, and J. B. Angell. Air analyzer fabricated on a silicon wafer. *IEEE Trans. Electron Devices*, ED-26:1880, 1979.

[3] S. Nakagawa, S. Shoji, and M. Esashi. A micro chemical analyzing system integrated on a silicon wafer. In *Proc. IEEE Micro Electro Mechanical Systems*, page 89, Napa Valley , CA, 1990.

[4] T. Ohnstein, T. Fukiura, J. Ridley, and U. Boone. Micromachined silicon microvalve. In *Proc. IEEE Micro Electro Mechanical Systems*, page 95, Napa Valley , CA, 1990.

[5] P. L. Bergstrom, J. Ji, Y. N. Liu, M. Kaviany, and K. D. Wise. Thermally driven phase-change microactuation. *J. Microelectromechanical Syms*, 4:10–17, 1995.

[6] M. A. Huff and M. A. Schmidt. Fabrication packaging and testing of a wafer-bonded microwafer. In *Proc. IEEE Solid State Sensor and Actuator Workshop*, pages 194–197, Hilton Head Island, SC, June 1992.

[7] M. A. Huff, M. S. Mettner, T. A. Lober, and M. A. Schmidt. A pressure-balanced electrically-actuated microvalve. In *Proc. IEEE Solid State Sensor and Actuator Workshop*, pages 123–127, Hilton Head Island, SC, June 1990.

[8] S.P. Timoshenko. *Theory of Plates and Shells.* McGraw-Hill, New York, 1940.

[9] J. J. Wortman and R. A. Evans. Young's modulus, shear modulus and poisson's ratio in silicon and germanium. *J. Appl. Phys.*, 36:153–156, 1965.

[10] B. R. Munson, D. F. Young, and T. H. Okiishi. *Fundamentals of Fluid Mechanics.* John Wiely & Sons, Inc., New York, 2 edition, 1994.